

## PROTON TOTAL CROSS SECTIONS ON $^1\text{H}$ , $^2\text{H}$ , $^4\text{He}$ , $^9\text{Be}$ , C AND O IN THE ENERGY RANGE 180 TO 560 MeV

P. SCHWALLER and M. PEPIN

*SIN, 5234 Villigen, Switzerland*

B. FAVIER <sup>†</sup> and C. RICHARD-SERRE <sup>††</sup>

*IPN, Université de Grenoble, France*

and

D. F. MEASDAY <sup>†††</sup> and P. U. RENBERG <sup>‡</sup>

*CERN, 1211 Genève 23, Switzerland*

Received 6 July 1978

**Abstract:** Proton total cross sections have been measured for the nuclei  $^1\text{H}$ ,  $^2\text{H}$ ,  $^4\text{He}$ ,  $^9\text{Be}$ , C and O from 180 to 560 MeV (610 to 1170 MeV/c). The standard transmission technique was used with a resulting total error of 1 % to 2 %. Statistical errors were small ( $< 1\%$ ) and the major contribution to the final error comes from uncertainties in applying the correction for Coulomb-nuclear interference in elastic scattering at small angles. For  $^4\text{He}$ ,  $^9\text{Be}$ ,  $^{12}\text{C}$  and  $^{16}\text{O}$  this experiment also gives new information on the real part of the spin-independent forward scattering amplitude for proton-nucleus elastic scattering. Total cross sections have been calculated using a Glauber model approach and poor agreement with the data is obtained, even for deuterium.

E

NUCLEAR REACTIONS  $^1\text{H}$ ,  $^2\text{H}$ ,  $^4\text{He}$ ,  $^9\text{Be}$ , C, O,  $E = 180\text{--}560$  MeV; measured  $\sigma(E)$ .  
Enriched and natural targets. Glauber model calculations.

### 1. Historical preamble

The experiment which we are about to describe has already been discussed at length in a thesis by one of the authors (P.S.) which was printed as a CERN report <sup>1)</sup>. Here we shall not go into great detail on the experimental technique nor on the analysis of the data, but we shall extend the discussion concerning the difficult problem of the systematic errors. We have also added data on  $^9\text{Be}$  which were not included in the earlier report. A preliminary account of our proton-proton results has already appeared <sup>2)</sup> but a slight correction to the data was made after this letter was published,

<sup>†</sup> Present address: Département de Physique Nucléaire et Corpusculaire, Université de Genève, 1211 Genève 4, Switzerland.

<sup>††</sup> Now attached to IN2P3; permanent address: CERN, 1211 Genève 23, Switzerland.

<sup>†††</sup> 1977–1978: visitor at DPh-N/HE, CEN Saclay; present permanent address: Physics Department, University of British Columbia, Vancouver BC, Canada V6T 1W5.

<sup>‡</sup> Present address: Gustaf Werner Institute, University of Uppsala, 75121 Uppsala, Sweden.

and so the values given in the CERN report <sup>1)</sup> were slightly different. Since that report was completed, it has become apparent that the Livermore phase shifts were not suitable for the Coulomb-nuclear interference in pp scattering. Now, in 1978, recent phase shifts and dispersion relations agree much better, so we have re-done the data analysis for the pp and pd total cross sections and so we present here a third (and final) set of values.

## 2. Introduction

Total cross sections have been of considerable use in many aspects of particle and nuclear physics. In the cases of proton-proton and proton-nucleus scattering at a few hundred MeV, the measurements are important as firm normalizations in phase-shift or optical model analyses. The confidence in total cross-section measurements stems from the simple experimental technique which is used, i.e. the method of counting the fraction of particles lost by scattering from a target. Accuracies of much better than 1 % can be achieved in certain circumstances, but for the case under discussion we shall see that difficulties exist at the level of 1 % to 2 %.

This experiment was undertaken because there existed a serious discrepancy in the total cross-section data for the proton-proton interaction between 500 and 700 MeV. There were many old results <sup>3-11)</sup> which were fairly consistent although errors were at times quite large (2 % to 20 %) and normally the Coulomb-nuclear interference correction had not been made, even though it varies between 1 % and 7 %. Then the high precision data of Bugg *et al.* <sup>12)</sup> were published with a relative precision of  $\pm 0.1$  % and an absolute precision of  $\pm 0.3$  % for most measurements, except for the lowest energy points which had slightly larger, but still impressive errors; i.e. at 516 MeV (1111 MeV/c) an absolute error of  $\pm 0.6$  % and at 656 MeV (1289 MeV/c) an absolute error of  $\pm 0.4$  %. However these points were, respectively, 9 % and 4 % higher than the general trend of the previous data. Now an experiment by Abrams *et al.* <sup>13)</sup> confirmed the pp total cross section of Bugg *et al.* at 2.2 GeV/c (3.0 GeV) to within 0.3 % [although there was an inconsistency in the pd total cross sections which was attributed in part to the problems of determining the density of liquid deuterium <sup>14)</sup>]. It thus seemed advisable to make a check of these lower energy pp measurements. After the completion of our experiment these two data points of Bugg *et al.* were withdrawn. We might also note that a similar problem exists at lower energies where the pp total cross sections of Goloskie and Palmieri <sup>15)</sup> between 70 and 147 MeV have been confirmed at 144 MeV by Cox *et al.* <sup>16)</sup> and at 68 MeV by Young and Johnston <sup>17)</sup> but are in serious disagreement with the value of Wigan *et al.* <sup>18)</sup> at 98 MeV.

The classical phase-shift analysis Livermore X [ref. <sup>19)</sup>] provided pp and np phase shifts up to 450 MeV. More recently this traditions has been continued by the group at the Virginia Polytechnic Institute (VPI) and there are now available analyses to 500 MeV for both pp (VPI 1) <sup>20)</sup> and np (VPI 2) <sup>21)</sup> phase shifts. Total

cross sections were not used in the original Livermore analyses but when our results became available they were incorporated in the data bank and the published VPI analyses include our data, however the impact was minimal because of the large number of other cross-section data already included.

For all published analyses, the values of  $\alpha = \text{Re}f(0^\circ)/\text{Im}f(0^\circ)$  disagreed with dispersion relation calculations. Recent phase-shift analyses at both Saclay <sup>22)</sup> and VPI <sup>23)</sup> are fairly different from the older versions and in much better agreement with dispersion relations and with each other. We have therefore used these new and as yet unpublished solutions to correct our data for the difficult extrapolation through the region of Coulomb-nuclear interference. The uncertainty in this correction remains as one of the largest errors.

We were also able to measure proton total cross sections for other light nuclei. When we started our experiment, there were few accurate nucleon-deuteron cross sections in our energy range, although new results for total nd cross sections from the Princeton-Pennsylvania Accelerator (PPA) have since been published <sup>24, 25)</sup>.

For the case of helium, no total cross-section data existed at a few hundred MeV for either neutrons or protons and our proton data are still the only ones available. For the nuclei beryllium, carbon and oxygen, there were many reasonable neutron total cross sections but few proton measurements and it was felt that some new proton measurements would make an interesting comparison with the neutron data, as well as providing a valuable check on the way we made the Coulomb-nuclear interference correction. Proton and neutron cross sections on  $I = 0$  nuclei (<sup>2</sup>H, <sup>4</sup>He, C, O, etc.) should be equal if charge symmetry of nuclear forces is valid, except that the Coulomb repulsion between the proton and the nucleus causes two effects: (i) the reduction of the effective energy in the scattering; (ii) a distortion of the incoming wave which reduces the cross section. These effects are small in our case but are several percent and easily observed for  $\pi$  total cross sections near the ( $\frac{3}{2}$ ,  $\frac{3}{2}$ ) resonance <sup>26, 27)</sup>. Now there are other tests of charge symmetry which are slightly more sensitive and these have recently been reviewed by Henley <sup>28)</sup>. These tests show that charge symmetry holds to about 1%. However we shall show that our results will provide useful supporting evidence at the level of about 5%.

We also attempted to measure the proton total cross sections for aluminium and copper but the Coulomb associated corrections, especially the Coulomb-nuclear interference correction, are so large that the results are not very valuable and so we have not included those data. It is still possible, however, to measure the total reaction cross sections in this energy region <sup>29)</sup> and this can then be combined with a measurement of the differential elastic scattering in a complete optical model analysis.

Glauber theory has been very successful in describing elastic scattering at small angles for high energies. It is interesting to investigate the validity of this model at lower energies where one would not expect the assumptions, which are made, to be correct. Surprisingly the model still works for the scattering of 100 to 300 MeV pions on nuclei. Very little has been done in nucleon-nucleus scattering at inter-

mediate energies, since the theory becomes more complicated when spin effects have to be considered. [Calculations have however been made using the Watson multiple-scattering optical potential <sup>30</sup>.] We have attempted to calculate the proton total cross sections on <sup>2</sup>H, <sup>4</sup>He, C and O, with Glauber theory making the simplest possible assumptions, and have then compared the calculations with our experimental data. The comparison shows that nucleon-alpha scattering is the most problematical, and that when that is understood the “3 $\alpha$ ” and “4 $\alpha$ ” nuclei of carbon and oxygen will be understood as well.

Forward dispersion relations (FDR) in nucleon-nucleus scattering provide a powerful tool for exploring the unphysical region of such a system, provided that experimental total cross-section data and real parts of the forward scattering amplitude are available. In particular FDR at intermediate energies are sensitive to meson exchange processes. Locher <sup>31</sup>) has performed an extension of a low-energy FDR analysis on <sup>4</sup>He to intermediate energies using our helium data.

### 3. Experimental technique

The experiment was carried out in the Proton Hall of the 600 MeV synchrotron at CERN. The configuration of the beam transport is illustrated in fig. 1. For most of the experiment we used a parasitic beam called the scattered out proton beam which is available through the normal extraction channel when another user is producing pions from an internal target. To obtain lower energies, a degrader of

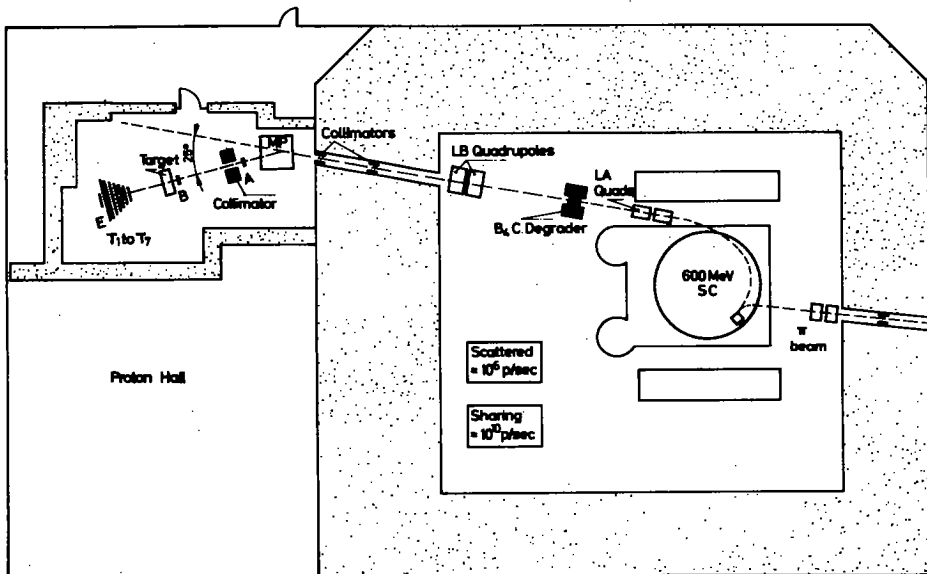


Fig. 1. Experimental lay-out at CERN SC.

boron carbide ( $B_4C$ ) was used. It was chosen because of its low  $Z$ , high density ( $2.5 \text{ g/cm}^3$ ) and low residual activity (apart from the 20 min  $^{11}C$  which quickly decays). For proton energies lower than 400 MeV, it was necessary to utilize the shared proton beam. This is a full energy beam ( $\approx 590 \text{ MeV}$ ) which was degraded and had an intensity which was kept at a few percent of the maximum available in the normal extracted beam.

After the degrader, the proton beam was refocused (sometimes defocused) by two quadrupole lenses, collimated in the shielding wall, analyzed in a  $25^\circ$  bending magnet and then defined with two counters, A and B, in coincidence. These plastic scintillation counters were 3 cm in diameter, 3 mm thick and placed 3 m apart.

TABLE I  
Target parameters

| Element                      | $^1H$ | $^2H$ | $^4He$ | $^9Be$ | C    | O ( $H_2O$ ) |
|------------------------------|-------|-------|--------|--------|------|--------------|
| Target length $l$ (cm)       | 75    | 35    | 75     | 5      | 5    | 8.7          |
| $\Delta l/l$ (%) $\pm$       | 0.2   | 0.3   | 0.2    | 0.1    | 0.1  | 0.25         |
| Thickness $th$ ( $g/cm^2$ )  | 5.3   | 5.9   | 9.3    | 9.3    | 9.2  | 8.7          |
| $\Delta th/th$ (%) $\pm$     | 0.21  | 0.5   | 0.21   | 0.1    | 0.15 | 0.3          |
| Absorption (%) at 200 MeV    | 7     | 10    | 13     | 14     | 12   | 12           |
| Energy loss (MeV) at 200 MeV | 52    | 25    | 37     | 34     | 38   | 40           |

All targets had absorptions ranging from 8% to 15%, the target-out absorption being always about 1.5%; (details are given in table 1). The cryogenic targets ( $H_2$ ,  $D_2$  and He) consisted of metal cylinders, 16 cm in diameter, with 0.25 mm thick mylar windows at both ends. Concentric copper cylinders with 15 cm diameter were mounted inside the liquid, and prevented bubbles produced on the outer walls from traversing the useful portion of the target. Thermal screens at liquid-nitrogen temperature surrounded the target at half distances to the cryostat vessel; these reduced the heat input considerably, resulting in an evaporation loss of liquid  $H_2$  and He of 0.1 litre/h and 1 litre/h, respectively.

Target densities were determined by measuring the vapour pressure of hydrogen and helium immediately above the liquid, and converting it into densities by means of tables <sup>32,33</sup>). The temperature of liquid deuterium was measured with a hydrogen gas thermometer, which was mounted inside the liquid, immediately above the target container. The observed temperatures varied between 21.4 K and 22.3 K, depending on whether the liquid hydrogen reservoir (20.4 K), the condenser of deuterium gas, was completely full or almost empty.

The detection system consisted of seven circular transmission counters, 5 mm thick, mounted on a trolley. The counters covered solid angles in the sequence 1, 2, 3, 4, 5, 7, 9, the smallest and largest counters being 15 and 45 cm in diameter, respectively. The whole assembly could be displaced on rails along the beam line.

The fast electronics consisted of standard NIM shapers and coincidence units and a SEN 300 scaler system (100 MHz). The pulses from the NIM shapers were between 4 and 6 nsec long, giving a resolution time in the coincidence of about 10 nsec. For a preselected number of monitor counts  $M = AB$ , all coincidences  $ABT_i$  ( $i = 1, \dots, 7$ ) were recorded simultaneously. A small counter E at the very back of the transmission counter assembly in coincidence with the monitor M measured the efficiency  $\varepsilon = ABT_iE/ABE$  in the centre of each counter  $T_i$ . For data taking it never dropped below 99.9%. The accidental counts never exceeded 0.2% of the real coincidences.

Efficiencies and accidental rates are sensitive to the intensity and duty cycle of the proton beam. The typical duty cycle of the proton beam was about 10% and intensities of less than 1000 protons/sec in AB were used to obtain the highest efficiency and the lowest accidental rate.

For each element and energy, transmission experiments were performed for two different distances between target centre and transmission counter array. This allowed us to cover the full interval of interest:

$$0.001 < |t| < 0.01 \text{ (GeV/c)}^2.$$

It also provided a cross check for systematic effects in the partial cross sections when different transmission counters covered the same solid angle  $\Omega$ .

Many tests were carried out in order to identify possible systematic errors. In particular, careful attention was given to any change of background absorption between target "in" and "out" measurements. To investigate this, we doubled this background absorption by inserting additional material in the beam line, in one case between counter B and the target, and in another test immediately in front of the transmission counters. Any systematic change in partial cross sections fell within statistical errors and therefore was negligible.

However, the background absorption, being different for each transmission counter  $T_i$ , depends on the kinetic energy of protons hitting the transmission counter array, and can be different for target "in" and "out" since the target itself causes an energy change. A usual target "out" experiment was compared with a background absorption obtained by degrading the proton beam in the SC machine hall with an additional block of material giving an energy loss equal to that of the target. We found that the correction to the partial cross sections was negligible for the smallest transmission counter, which was closest to the target, but increased towards the big counters. This is probably due to the energy dependence of secondary reactions in the counter array. A small correction ( $\leq 0.3\%$ ) was applied.

As a simple method of deriving the mean energy of the proton beam, we used the differential range curve technique. The mean kinetic energy of the proton beam is found from the position of the stopping peak using range-energy tables and can be determined to within  $\pm 2$  MeV. We used the range-energy tables of Serre<sup>34)</sup> which agree to within the claimed error with those of Janni<sup>35)</sup> and of Barkas and Berger<sup>36)</sup>.

In order to get an idea of possible systematic errors in the range-energy method,

we performed a floating-wire experiment in the bending magnet. A systematic discrepancy of at most 3 MeV was observed between the floating-wire technique and the range curves.

#### 4. Data evaluation

As Coulomb and Coulomb-nuclear interference scattering cross sections are infinite at zero angle, corrections for these effects must be applied before making the extrapolation to zero solid angle. Thus we correct all the measured partial cross sections in the following way. The fraction of protons which were scattered outside the solid angle  $\Omega$  by single, plural and multiple Coulomb scattering was calculated and the correction applied to each partial cross section  $\sigma(\Omega)$ . The Coulomb-nuclear interference effect and the extrapolation to zero solid angle were treated differently for the lightest nuclei ( $^1\text{H}$  and  $^2\text{H}$ ) and for the complex nuclei (He, Be, C, O).

Now the cross section for the elastic scattering of protons off nuclei is given by

$$\left(\frac{d\sigma}{d\Omega}\right) = \left(\frac{d\sigma}{d\Omega}\right)_C + \left(\frac{d\sigma}{d\Omega}\right)_N + \left(\frac{d\sigma}{d\Omega}\right)_I \quad (1a)$$

(C = Coulomb, N = nuclear, I = interference), where

$$\left(\frac{d\sigma}{d\Omega}\right)_I = 2(\text{Re } f_C \text{ Re } f_N + \text{Im } f_C \text{ Im } f_N), \quad (1b)$$

where  $f_N$ , the nuclear amplitude is approximated by

$$f_N = \frac{ik}{4\pi} \sigma_T (1 - i\alpha) e^{\lambda\gamma^2 t}, \quad (1c)$$

and  $f_C$  is given by

$$f_C = -\frac{\eta_C}{2k \sin^2 \frac{1}{2}\theta} \exp[-i\delta_B F(t)], \quad (1d)$$

where  $\eta_C = (Z/\beta) (e^2/\hbar c)$ ,  $\delta_B$  is the Bethe phase <sup>71)</sup>, and  $F(t) = \exp(-\frac{1}{6}R^2|t|)$ , the form factor. Values of  $R$  and  $\gamma^2$  are listed in table 2.

TABLE 2  
Parameters used in correction of data for extrapolation

| Target                          | $^1\text{H}$ | $^2\text{H}$ | $^4\text{He}$ | $^9\text{Be}$ | $^{12}\text{C}$ | $^{16}\text{O}$ |
|---------------------------------|--------------|--------------|---------------|---------------|-----------------|-----------------|
| $R$ (fm)                        | a)           | 2.8 b)       | 1.67 c)       | 2.15          | 2.4 d)          | 2.54            |
| $\gamma^2$ (GeV/c) <sup>2</sup> |              |              | 27            | 60            | 70              | 84              |

a) The form factor in the pp data evaluation was neglected.

b) Franco and Glauber <sup>64)</sup>.

c) Frosch *et al.* <sup>73)</sup>.

d) Bethe <sup>71)</sup>.

Since  $f_C$  is essentially real,  $\text{Re}f_C \text{Re}f_N$  provides the dominant contribution to the interference correction. This is true as long as the quantity  $\alpha = \text{Re}f_N / \text{Im}f_N$  is bigger than  $|0.02|$ . However,  $\text{Re}f_N$  is, at present, poorly known in the energy region we are considering. Of course  $\text{Im}f_N$  is known from the optical theorem. Now it is easy to show that

$$\text{Re} f_C \text{Re} f_N \propto \frac{\alpha \sigma_T Z}{t}. \quad (2)$$

The  $Z$ -dependence tells us that any structure in the Coulomb corrected partial cross sections will be easier to detect in the heavier elements. Since we took partial cross sections at many angles, we have effectively measured the integrated differential elastic scattering cross sections throughout the Coulomb-nuclear interference region. Because of the unique  $t$  (or  $\theta$ ) dependence of the interference effect it is possible to extract  $\alpha$  from our data. Since the precision of the partial cross sections in this experiment is limited to 0.3% by statistical and systematic errors, it was possible to extract  $\alpha$  for only He, Be, C and O.

A similar discussion of Coulomb-nuclear interference effects has been made recently by Cooper and Johnson<sup>72)</sup> but their methods are needed for rather extreme cases where the effects are very large, thus they take as an example the scattering of 50 MeV pions off lead. For our case their method reduces to the present technique of polynomial extrapolation.

Fig. 2 shows a typical example of the extrapolation technique.

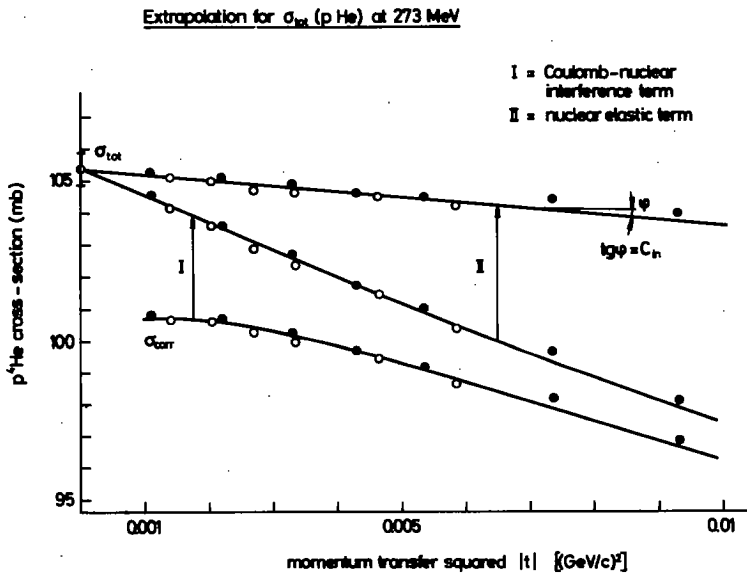


Fig. 2. Typical extrapolation for  $p^4\text{He}$  data where  $\sigma_{\text{corr}}$  is the experimental datum after it has been corrected for single and multiple Coulomb scattering.

Extrapolation for  $\sigma_{tot}(pp)$  at 268 MeV

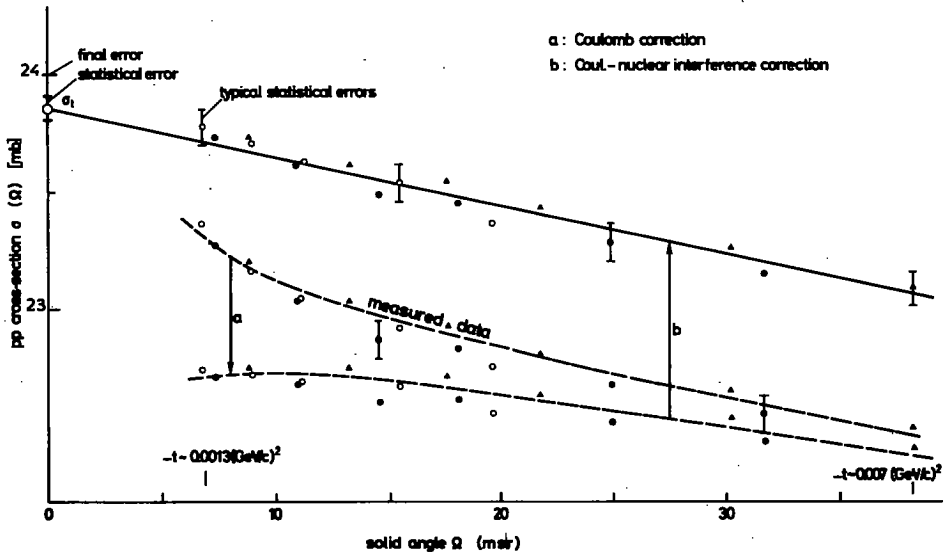


Fig. 3. Typical extrapolation for pp data.

For the analysis of the hydrogen and deuterium data we calculated the interference term using the nucleon-nucleon phase shifts from the Saclay analyses<sup>22</sup>), and a typical extrapolation is shown in fig. 3.

To illustrate the reason for the change in the Coulomb-nuclear interference correction from the CERN report we show in fig. 4 the values of  $\alpha$  given by several phase-shift analyses as well as those from the dispersion relation calculation of Grein<sup>37</sup>).

We see that in our energy region the values of  $\alpha_{pp}$  from phase-shift analyses have increased considerably with time. The Livermore analysis has the lowest value, the published solution VPI 1 is intermediate and the latest unpublished solution VPI 3 is highest, but now there is excellent agreement between this new analysis, the Saclay analysis and the dispersion relation calculation of Grein. We note that the recent analyses include many more experimental data, in particular the differential cross-section measurements of proton-proton scattering at small angles made by the Geneva group at CERN<sup>38</sup>) and so the values of  $\alpha$  should be much more reliable. Less information is available for np scattering but we have assumed that the Livermore np analysis is also low and have therefore used the only other available values, those of Grein<sup>37</sup>).

The nuclear scattering of a proton on a deuteron can be described to a good approximation with multiple scattering theory, provided that the energy of the incident proton is high enough, i.e. the de Broglie wavelength  $\lambda$  is small with respect to the r.m.s. radius  $R$  of the deuteron. This condition is satisfied in our energy region

$$\lambda \approx 0.2 \ll R \approx 2.8 \text{ fm.}$$

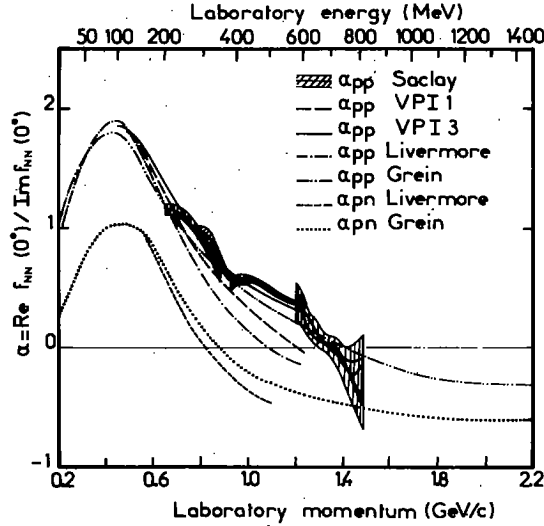


Fig. 4. Values of  $\alpha = \text{Re}f(0^\circ)/\text{Im}f(0^\circ)$  for nucleon-nucleon scattering at a few hundred MeV. Note that the recent pp phase-shift analyses<sup>22,23</sup> agree with the dispersion relation calculation of Grein<sup>37</sup>), but are significantly higher than the published VPI<sup>20</sup>) and Livermore<sup>19</sup>) analyses. We use the Saclay analysis for the pp Coulomb-nuclear interference correction. Note that between 600 and 800 MeV there are four Saclay solutions.

In the very small angle scattering limit, the incident proton has a large impact parameter and therefore essentially scatters from one nucleon only. According to the impulse-approximation, the spin-independent single scattering pd amplitude is the coherent sum of the Coulomb amplitude  $f_C$  and the spin-independent proton-proton and proton-neutron amplitude  $f_{pp}$  and  $f_{pn}$ , where  $f_{pp}$  still contains Coulomb phases:

$$f_{pd}^C = (f_C + f_{pp} + f_{pn})F(t), \quad (3)$$

where  $F(t)$  is the deuteron form factor, which is assumed to be equal for  $f_C$  and  $f_{pp}$  ( $f_{pn}$ ), and which drops very fast with increasing  $|t|$  because of the weak binding and the relatively large distance between the two nucleons in the deuteron.

In this approach  $f_C$  interferes with

$$f_{pd} = f_{pp} + f_{pn}, \quad (4)$$

resulting in an interference cross section

$$\left(\frac{d\sigma}{d\Omega}\right)_I(\text{pd}) = 2 \text{Re}(f_C f_{pd}^*) F^2. \quad (5)$$

The amplitude  $f_{pn}$  also was obtained using Grein's value for  $\alpha_{np}$ .  $\alpha_{nd}$  is given later in table 4.

We shall see that the interference correction dominates all other problems both

in the statistical fitting of the various functions, but more important, in the basic formulation of the fitting procedure. This is true for all the nuclei herein described, though the details of this interference correction are quite different for the three cases, hydrogen, deuterium and light complex nuclei.

However we shall briefly discuss the other errors to illustrate the potential accuracy of this type of experiment. Fairly minor contributions come from counting statistics ( $\pm 0.2\%$ ), stability of the efficiency of the scintillation counters ( $\pm 0.05\%$ ), accidental coincidences ( $\pm 0.1\%$ ) uncertainties in the background correction ( $\pm 0.15\%$ ) and target length ( $\pm 0.2\%$ ) (except for deuterium where we take  $\pm 0.5\%$  because of the temperature uncertainty). The energy measurement when converted to an error in the cross section is normally negligible ( $\leq 0.2\%$ ), except for the energy region between 400 and 600 MeV where it reaches  $\pm 0.3\%$  for the pd cross sections and  $\pm 0.6\%$  for the pp cross sections.

For the Coulomb-nuclear interference correction for the pp and pd case we shall take the correction from the Saclay phase shifts. We shall assume that the error on this correction is the difference between the cross sections obtained in our CERN report <sup>1)</sup> (using the Livermore phase shifts) and the present values, i.e.  $0.8\%$  depending somewhat on the energy for the pp case and about  $0.5\%$  for the pd case.

For the nuclei <sup>4</sup>He, <sup>9</sup>Be, C and O the error on the interference correction depends on two factors; uncertainties in the parameters used in the analysis and statistical errors in the fitting procedure. We take the following parameter uncertainties:

|   |                                       |
|---|---------------------------------------|
| kinetic energy of proton:                 | $\delta E = \pm 2 \text{ MeV},$       |
| r.m.s. radius of the nucleus:             | $\delta R/R = \pm 10\%,$              |
| slope parameter in elastic cross section: | $\delta\gamma^2/\gamma^2 = \pm 20\%.$ |

We obtain the following systematic errors:

$$\frac{\delta\sigma_T}{\sigma_T} = \pm 0.6\%, \quad \delta\alpha = \begin{cases} \pm 0.13, & \text{at 200 MeV} \\ \pm 0.07, & \text{at 550 MeV.} \end{cases}$$

The statistical errors in the fitting procedure are typically as follows:

$$\frac{\delta\sigma_T}{\sigma_T} = \pm(1 \text{ to } 3)\%, \quad \delta\alpha = \pm(0.1 \text{ to } 0.15).$$

### 5. Results and discussions

We present our results both numerically in tables 3 to 8 and graphically in figs. 5-11. We include the data for the proton total cross sections on <sup>1</sup>H, <sup>2</sup>H, <sup>4</sup>He, <sup>9</sup>Be, C and O, together with the ratio of the real to the imaginary part of the proton nucleus forward scattering amplitude. Previous experimental data plotted in the figures have been taken from various compilations <sup>3, 46-49)</sup> as well as data missed by, or post-dating such compendia [refs. <sup>16-18, 24, 25, 40-47)</sup>].

In fig. 6 [ $\sigma_T(\text{pd})$ ] we have included only the most recent data because they extend

TABLE 3  
Results for pp total cross sections

| Lab kinetic energy (MeV) | Lab momentum (MeV/c) | $\sigma_T$ (pp) (mb) | Statistical error $\pm \delta\sigma_T$ (mb) | Total error $\pm \delta\sigma$ (mb) | $\Delta\sigma_{\text{CNI}}^*)$ (mb) |
|--------------------------|----------------------|----------------------|---|-------------------------------------|-------------------------------------|
| 179.0                    | 607                  | 24.20                | 0.12  | 0.24                                | 1.65                                |
| 267.5                    | 757                  | 23.85                | 0.10  | 0.23                                | 0.90                                |
| 342.5                    | 872                  | 24.55                | 0.10  | 0.23                                | 0.58                                |
| 388.0                    | 937                  | 25.70                | 0.10  | 0.23                                | 0.50                                |
| 406.5                    | 963                  | 26.50                | 0.10  | 0.23                                | 0.40                                |
| 439.5                    | 1009                 | 27.95                | 0.14  | 0.29                                | 0.35                                |
| 502.5                    | 1093                 | 31.25                | 0.15  | 0.34                                | 0.28                                |
| 513.5                    | 1108                 | 31.95                | 0.19  | 0.36                                | 0.27                                |
| 555.0                    | 1162                 | 34.80                | 0.24  | 0.39                                | 0.22                                |

\*)  $\Delta\sigma_{\text{CNI}}$ , the interference correction, i.e. the difference between the quoted value of  $\sigma_T$  and the value obtained when no Coulomb-nuclear interference correction is made before extrapolation.

TABLE 4  
Results for pd total cross sections and the resulting Glauber correction together with the np cross section used in the calculation

| Lab kinetic energy (MeV) | Lab momentum (MeV/c) | $\sigma_T$ (pd) (mb) | Total error $\pm \delta\sigma$ (mb) | $\alpha_{\text{nd}}$ | $\sigma_{\text{np}}$ (mb) | Glauber correction $\Delta\sigma$ (mb) |
|--------------------------|----------------------|----------------------|-------------------------------------|----------------------|---------------------------|--|
| 227                      | 691                  | 63.2                 | 0.7                                 | 0.76                 | 42.0                      | $2.5 \pm 1.5$                          |
| 275                      | 769                  | 60.8                 | 0.7                                 | 0.54                 | 38.6                      | $1.5 \pm 1.5$                          |
| 348                      | 880                  | 59.9                 | 0.7                                 | 0.26                 | 34.0                      | $-1.1 \pm 1.5$                         |
| 412                      | 971                  | 61.3                 | 0.7                                 | 0.10                 | 33.8                      | $-0.7 \pm 1.5$                         |
| 422                      | 985                  | 61.3                 | 0.7                                 | 0.09                 | 33.8                      | $-0.5 \pm 1.5$                         |
| 483                      | 1067                 | 64.6                 | 0.7                                 | 0.05                 | 34.0                      | $-1.1 \pm 1.5$                         |
| 560                      | 1168                 | 69.4                 | 0.7                                 | 0.00                 | 35.4                      | $0.9 \pm 1.5$                          |

\*) Error for the Glauber correction is dominated by discrepancies in  $\sigma(\text{np})$ , see fig. 12.

TABLE 5  
Results for the p<sup>4</sup>He total cross sections

| Lab kinetic energy (MeV) | Lab momentum (MeV/c) | $\sigma_T$ (mb) | Total error $\pm \delta\sigma_T$ (mb) | $\alpha \pm \delta\alpha$ | " $\alpha$ " (smoothed curve) | " $\sigma_T$ " (mb) |
|--------------------------|----------------------|-----------------|---------------------------------------|---------------------------|-------------------------------|---------------------|
| 224                      | 686                  | 106.3           | 1.3                                   | $0.48 \pm 0.17$           | 0.73                          | 109                 |
| 273                      | 765                  | 105.7           | 1.3                                   | $0.52 \pm 0.18$           | 0.52                          | 106                 |
| 345                      | 875                  | 106.8           | 1.1                                   | $0.29 \pm 0.16$           | 0.30                          | 107                 |
| 413                      | 972                  | 110.8           | 1.2                                   | $0.17 \pm 0.18$           | 0.20                          | 111                 |
| 430                      | 996                  | 112.8           | 1.0                                   | $0.16 \pm 0.16$           | 0.18                          | 113                 |
| 491                      | 1078                 | 117.6           | 1.5                                   | $0.14 \pm 0.24$           | 0.10                          | 117                 |
| 563                      | 1172                 | 123.7           | 0.9                                   | $0.09 \pm 0.14$           | 0.02                          | 123                 |

TABLE 6  
Results for the p<sup>9</sup>Be total cross sections

| Lab kinetic energy (MeV) | Lab momentum (MeV/c) | $\sigma_T$ (mb) | Total error $\pm \delta\sigma_T$ (mb) | $\alpha \pm \delta\alpha$ |
|--------------------------|----------------------|-----------------|---------------------------------------|---------------------------|
| 225                      | 668                  | 235.7           | 5.2                                   | 0.64 ± 0.18               |
| 279                      | 776                  | 229.3           | 4.8                                   | 0.50 ± 0.16               |
| 350                      | 883                  | 231.5           | 3.8                                   | 0.36 ± 0.14               |
| 394                      | 946                  | 238.6           | 3.4                                   | 0.28 ± 0.13               |
| 445                      | 1016                 | 244.4           | 3.4                                   | 0.20 ± 0.12               |
| 466                      | 1045                 | 248.0           | 3.1                                   | 0.17 ± 0.10               |
| 518                      | 1114                 | 254.0           | 2.6                                   | 0.13 ± 0.10               |
| 557                      | 1164                 | 259.3           | 2.5                                   | 0.11 ± 0.09               |

TABLE 7  
Results for the p<sup>12</sup>C total cross sections

| Lab kinetic energy (MeV) | Lab momentum (MeV/c) | $\sigma_T$ (mb) | Total error $\pm \delta\sigma_T$ (mb) | $\alpha \pm \delta\alpha$ | " $\alpha$ " (smoothed curve) | " $\sigma_T$ " (mb) |
|--------------------------|----------------------|-----------------|---------------------------------------|---------------------------|-------------------------------|---------------------|
| 191                      | 627                  | 282             | 9                                     | 0.44 ± 0.19               | 0.78                          | 305                 |
| 223                      | 684                  | 275             | 12                                    | 0.35 ± 0.29               | 0.65                          | 290                 |
| 277                      | 772                  | 283             | 4                                     | 0.50 ± 0.11               | 0.46                          | 281                 |
| 306                      | 817                  | 288             | 6                                     | 0.47 ± 0.19               | 0.38                          | 284                 |
| 348                      | 880                  | 286             | 6                                     | 0.29 ± 0.18               | 0.30                          | 286                 |
| 349                      | 881                  | 283.5           | 3                                     | 0.21 ± 0.09               | 0.30                          | 286                 |
| 372                      | 914                  | 297             | 4.5                                   | 0.38 ± 0.14               | 0.26                          | 293                 |
| 392                      | 944                  | 300.5           | 4                                     | 0.39 ± 0.12               | 0.22                          | 295                 |
| 441                      | 1011                 | 298             | 5                                     | 0.11 ± 0.14               | 0.16                          | 299                 |
| 453                      | 1027                 | 302             | 7                                     | 0.10 ± 0.19               | 0.14                          | 303                 |
| 456                      | 1031                 | 301             | 7                                     | 0.09 ± 0.14               | 0.14                          | 304                 |
| 467                      | 1046                 | 308             | 4                                     | 0.11 ± 0.10               | 0.13                          | 309                 |
| 497                      | 1086                 | 314             | 8                                     | 0.14 ± 0.15               | 0.09                          | 312                 |
| 506                      | 1098                 | 313             | 4                                     | 0.06 ± 0.09               | 0.08                          | 314                 |
| 518                      | 1113                 | 319             | 4.5                                   | 0.16 ± 0.09               | 0.07                          | 315                 |
| 553                      | 1159                 | 323             | 10                                    | 0.03 ± 0.16               | 0.04                          | 324                 |
| 559                      | 1167                 | 327             | 6                                     | 0.11 ± 0.12               | 0.03                          | 322                 |
| 463                      | 1041                 | 301             | 8 *)                                  | 0.21 ± 0.14               | 0.13                          | 299                 |
| 502                      | 1093                 | 313             | 5 *)                                  | 0.06 ± 0.09               | 0.09                          | 318                 |
| 550                      | 1155                 | 323             | 11 *)                                 | 0.00 ± 0.16               | 0.04                          | 324                 |

\*) Data measured with CH<sub>2</sub> target; evaluation similar to that for oxygen.

over larger energy ranges, and are of higher precision. In figs. 10 and 11 we distinguish simply between the proton and neutron cross sections on carbon and oxygen in order to get an impression of the validity of charge symmetry.

TABLE 8  
Results for the  $p^{16}\text{O}$  total cross sections

| Lab kinetic energy (MeV) | Lab momentum (MeV/c) | $\sigma_T$ (mb) | Total error $\pm \delta\sigma_T$ (mb) | $\alpha \pm \delta\alpha$ | " $\alpha$ " (smoothed curve) | " $\sigma_T$ " (mb) |
|--------------------------|----------------------|-----------------|---------------------------------------|---------------------------|-------------------------------|---------------------|
| 190                      | 627                  | 387             | 30                                    | $0.78 \pm 0.31$           | 0.87                          | 394                 |
| 222                      | 682                  | 386             | 15                                    | $0.74 \pm 0.21$           | 0.67                          | 380                 |
| 276                      | 770                  | 360             | 7                                     | $0.50 \pm 0.12$           | 0.46                          | 357                 |
| 348                      | 880                  | 367             | 6                                     | $0.36 \pm 0.12$           | 0.30                          | 364                 |
| 392                      | 943                  | 377             | 6                                     | $0.24 \pm 0.11$           | 0.23                          | 377                 |
| 442                      | 1012                 | 381             | 6                                     | $0.12 \pm 0.11$           | 0.16                          | 383                 |
| 516                      | 1111                 | 397             | 4                                     | $0.10 \pm 0.08$           | 0.07                          | 397                 |
| 558                      | 1165                 | 411             | 7                                     | $0.04 \pm 0.09$           | 0.03                          | 410                 |

### 5.1. PROTON-PROTON DATA

In fig. 5 our pp total cross-section data are compared to other data as well to the three phase-shift analyses VPI 1 [ref. <sup>20</sup>], VPI 3 [ref. <sup>23</sup>] and Saclay <sup>22</sup>). The agreement with the analyses is good, especially VPI 3. We have plotted the total cross section extrapolated to zero solid angle. For low energies it is common to quote the total elastic cross section for angles greater than a certain value, often  $12^\circ$  as this angle is in the middle of the interference dip. For consistency in the diagram

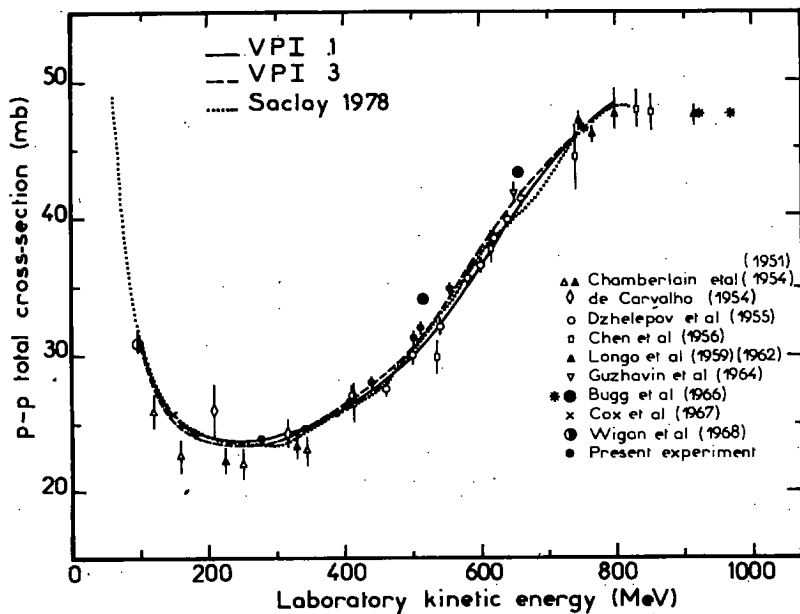


Fig. 5. Total cross-section data for pp compared to three recent phase-shift analyses. Note that the data of Bugg *et al.* at 516 and 656 MeV (circled) have been withdrawn. The data of Wigan and Cox have been corrected to give the *total* cross section.

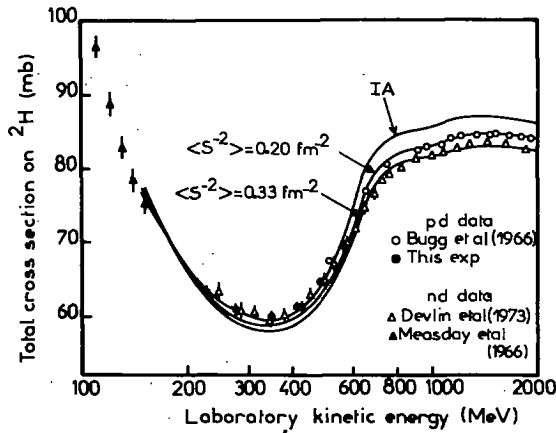


Fig. 6. Neutron and proton total cross sections for deuterium. Note the agreement in our energy region. The data of Bugg *et al.* seem to have a systematic error.

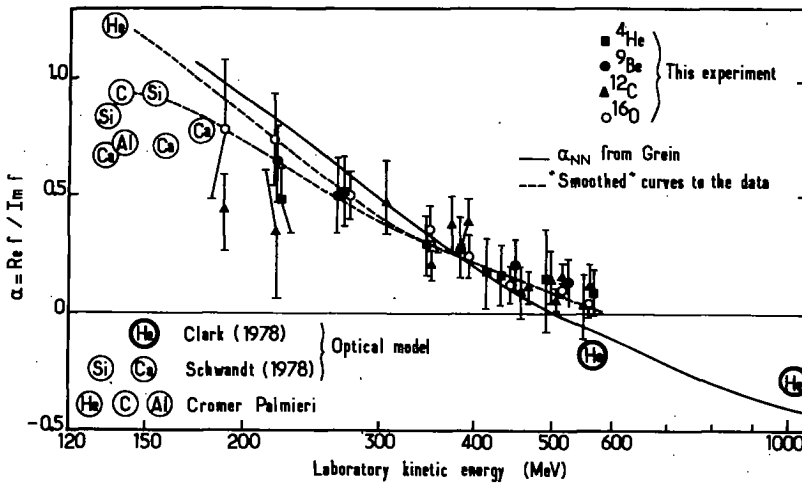


Fig. 7: Comparison of  $\alpha = \text{Re} f(0^0)/\text{Im} f(0^0)$  from various optical model analyses<sup>48,49,54</sup> with the present data (numerical values are listed in table 9). Note that  $\alpha$  from Grein (average of  $\alpha_{pp}$  and  $\alpha_{pn}$ ) follows the general trend. The smoothed curves were used to obtain our best estimate for  $\sigma_T$ , upper curve for He, lower curve for the other elements.

we have therefore corrected the results of Cox *et al.*<sup>16</sup>) at 144 MeV from 24.0 to 25.7 mb (+7%) and the result of Wigan *et al.*<sup>18</sup>) at 98 MeV from 28.5 to 30.8 mb (+8%). These corrections were estimated from phase-shift analyses at nearby energies, not the exact energies, and have an uncertainty of 1 or 2%.

We agree with most of the previous measurements of the pp total cross section although many of them are 5 to 10 times less accurate. However we disagree with the datum of Bugg *et al.*<sup>12</sup>) at 516 MeV by about 2.1 mb (7%) of which approximately

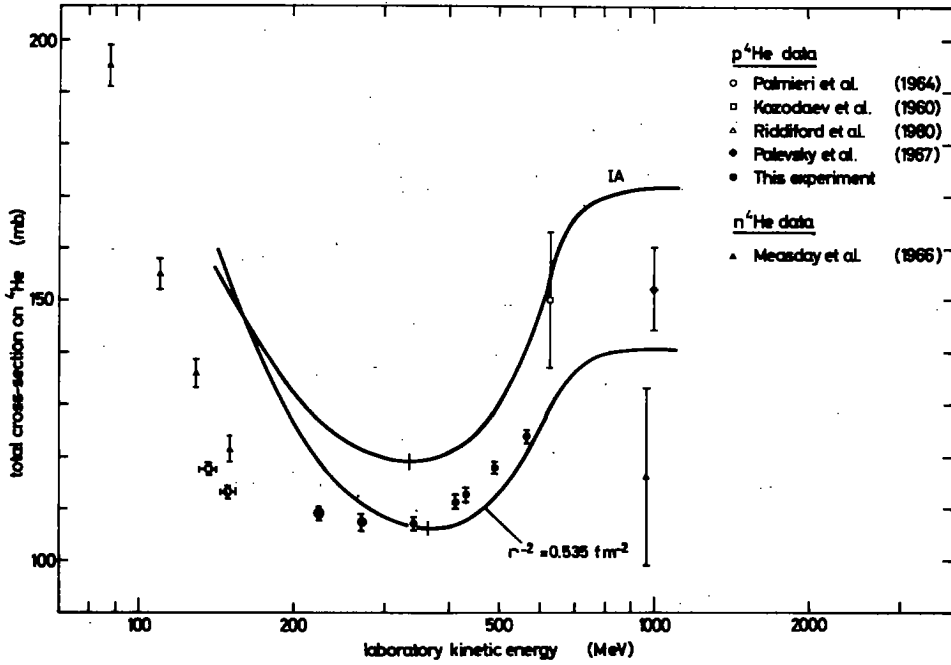


Fig. 8. Total cross sections for protons and neutrons on  ${}^4\text{He}$ . Note that a simple-minded Glauber calculation (full-line) does not fit the data, see text.

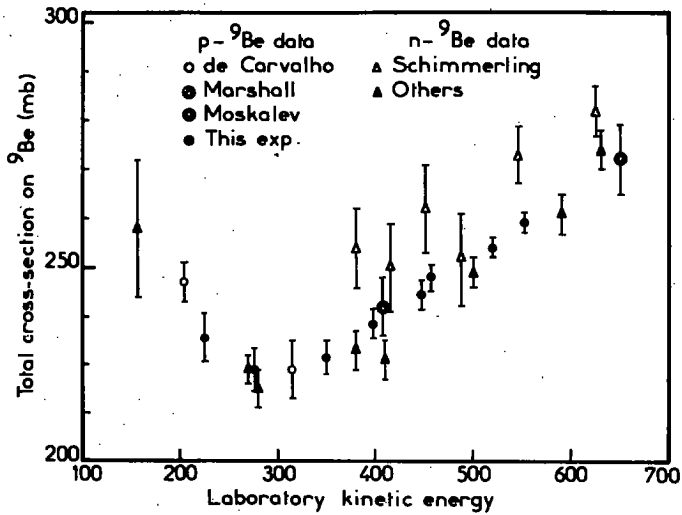


Fig. 9. Total cross sections for protons and neutrons on  ${}^9\text{Be}$ .

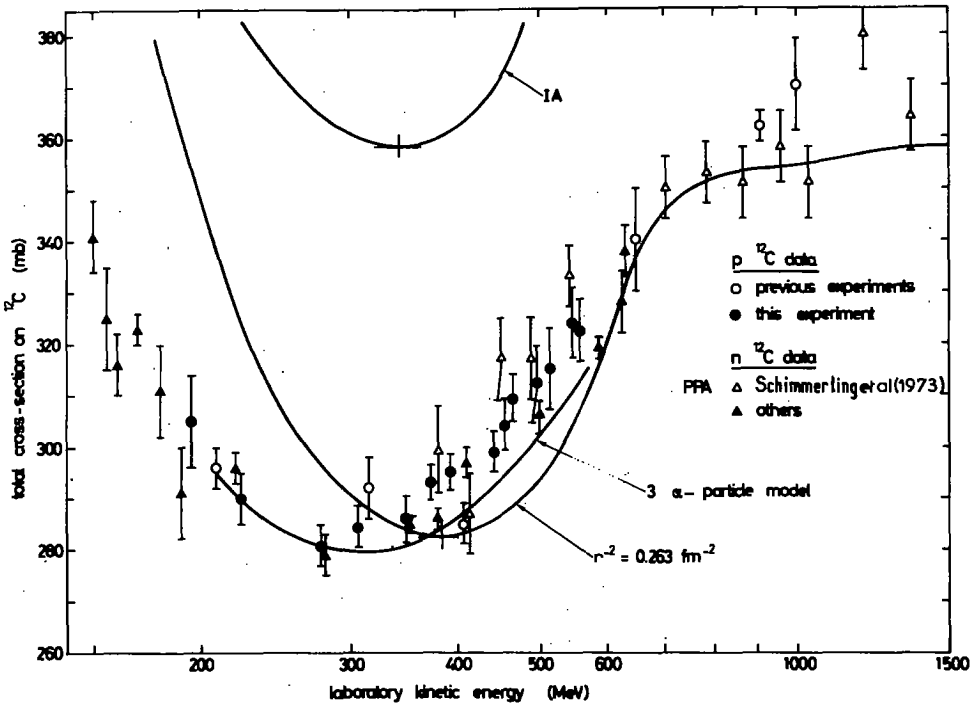


Fig. 10. Total cross sections for protons and neutrons on  $^{12}\text{C}$ .

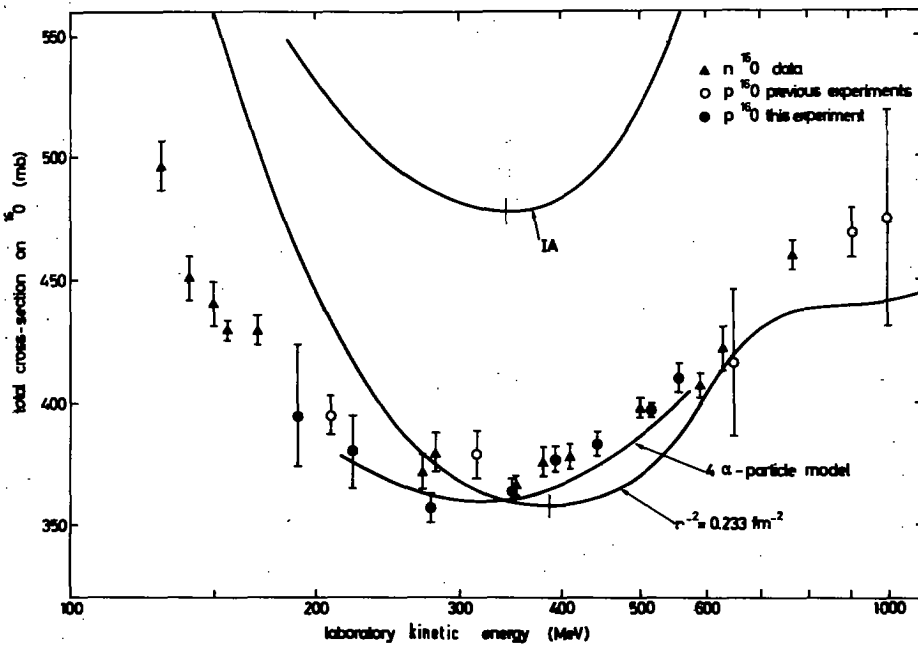


Fig. 11. Total cross sections for protons and neutrons on  $^{16}\text{O}$ .

0.45 mb is due to the difference in the interference correction. Bugg *et al.* based their correction on older versions of forward dispersion relations. We have preferred to use a more phenomenological approach using phase-shift analyses but these two methods now agree quite well. We note that Bugg has recently withdrawn the two lowest energy points (516 and 656 MeV) because of some problems in the extrapolation procedure<sup>39)</sup>. The other points are still valid and are in excellent agreement with other high-energy experiments.

## 5.2. PROTON-DEUTERON DATA

In fig. 6 our pd data are presented together with the most recent measurements<sup>12, 25, 44)</sup> of other nucleon-deuteron total cross sections in our energy region. We note that there is excellent agreement between our results and the nd data of Devlin *et al.*<sup>25)</sup>. At higher energies however their data are about 1.2 mb lower than the pd data of Bugg *et al.*<sup>12)</sup> but, as we have already noted, at 3 GeV/c the pd data of Abrams<sup>13)</sup> are also below the data of Bugg *et al.*, by a similar amount. We have performed some Glauber model calculations to attempt to fit the data and we shall discuss these later with the other nuclei.

## 5.3. PROTON-NUCLEUS DATA

Because of its effect on the total cross section we shall discuss, first of all, our values for  $\alpha$ . We compare them in fig. 7 with the values of  $\alpha_{NN}$  from the dispersion relation calculations of Grein and we see that the general trend of the points is followed quite well. Because there is a considerable scatter amongst our points, especially below 300 MeV, it seemed wise to use a smoothed value of  $\alpha$ . To anchor the curves at about 150 MeV we have used the optical model analyses of Schwandt<sup>48)</sup> together with the analysis of small angle proton nucleus scattering by Cromer and Palmieri<sup>49)</sup>, later improved by Jarvis<sup>50)</sup> and again by Jarvis *et al.*<sup>51)</sup>. For completeness we also give the results of optical model analyses of helium at higher energies<sup>52, 54)</sup>. As there is a significant trend for  $\alpha$  to be smaller for heavier nuclei we have used two curves below 300 MeV, the upper one for helium and the lower one for all the other elements.

Now in the Born approximation [see Schiff<sup>55)]</sup>

$$\alpha = \frac{\text{Re } f(0^\circ)}{\text{Im } f(0^\circ)} = \frac{V r_R^3}{W r_I^3} = \frac{J_R}{J_I}, \quad (6)$$

where  $V$  and  $W$  are the depths of the real and imaginary parts, respectively, of a square well potential of radius  $r$ ;  $J_R$  and  $J_I$  are the volume integrals of the real and imaginary parts of the potential. We give in table 9 the results of these analyses and it is clear that although relation (6) holds approximately at higher energies for helium, around 150 MeV it is not adequate for our purposes and the value of  $\alpha$  must be calculated correctly. We note that some optical model analyses such as

TABLE 9  
Values of  $\alpha$  from analyses of differential cross-section data

| Author                             | Element | Proton energy<br>(MeV) | $\alpha = \frac{\text{Re}f(0^\circ)}{\text{Im}f(0^\circ)}$ | $\frac{J_R}{J_I}$ |
|------------------------------------|---------|------------------------|--|-------------------|
| Cromer and Palmieri <sup>49)</sup> | He      | 140                    | 1.23   |                   |
|                                    | Be      | 140                    | 0.90   |                   |
|                                    | C       | 140                    | 0.92   |                   |
|                                    | Al      | 140                    | 0.71   |                   |
| Schwandt <sup>48)</sup>            | Si      | 80                     | 0.74   | 3.60              |
|                                    | Si      | 135                    | 0.85   | 1.83              |
|                                    | Si      | 155                    | 0.93   | 2.10              |
| Schwandt <sup>48)</sup>            | Ca      | 80                     | 0.51   | 3.00              |
|                                    | Ca      | 135                    | 0.68   | 1.76              |
|                                    | Ca      | 160                    | 0.72   | 1.67              |
|                                    | Ca      | 181                    | 0.78   | 1.70              |
| Clark <sup>54)</sup>               | He      | 561                    | -0.167   | -0.193            |
|                                    | He      | 1029                   | -0.279   | -0.286            |

that by Ingemarsson and Tibell <sup>56)</sup> do not have a consistent trend for  $J_R/J_I$  as a function of nuclear mass, so some caution must be used.

It is important to remember that  $\alpha$  can be of interest itself. Ray and Coker <sup>57)</sup> have investigated nucleon-nucleus scattering and they find that  $\alpha$  is a good indicator. Eckart and Weigel <sup>58)</sup> have also studied optical model potentials in this energy region using dispersion relations and the real part of the potential is again problematic.

The total cross-section data are plotted in figs. 8-11 and compared to previous proton and neutron data. For helium there are no data at a few hundred MeV, although we can note reasonable continuation to the neutron-helium data between 77 and 151 MeV [ref. <sup>44)</sup>]. The proton-helium total cross sections of Palmieri and Goloskie <sup>59)</sup> still seem a little low.

For beryllium there is a slight discrepancy. As  $\sigma_T(\text{nn})$  is about 10 mb less than  $\sigma_T(\text{np})$  in our energy region, it is reasonable to expect that the total cross section for neutrons on  $^9\text{Be}$  should be a few mb lower than for  $p^9\text{Be}$ . Our data agree well with older proton measurements and are systematically a few mb above the old neutron data. However the recent neutron data of Schimmerling *et al.* <sup>46,47)</sup> lie significantly above our data ( $\approx 10$  mb) which is somewhat disconcerting. Because of this discrepancy between the data, we strongly recommend a remeasurement of the neutron cross sections. Note that fig. 2 of ref. <sup>46)</sup> illustrates how this discrepancy between Schimmerling *et al.* and older data is there for only Be, Cu and U, and not for the other nine elements. We feel that this problem is well worth a reinvestigation because it reflects on the comparison we make for charge symmetry.

For carbon and oxygen our data agree with previous proton as well as neutron

cross sections. It is interesting to note that the present proton data are as accurate as the neutron data in this energy region even though a measurement of total neutron cross sections is intrinsically easier.

#### 5.4. CALCULATION OF $\sigma_T$ BY GLAUBER THEORY

Multiple scattering theory has been applied extensively during the last few years and successfully describes the structure of pion- or proton-nucleus differential cross sections at high energies, in the limit of geometrical optics

$$kR \gg 1,$$

where  $R$  is the r.m.s. radius of the nucleus, and  $k$  is the beam momentum. Wilkin<sup>60)</sup> has investigated the low-energy region where the model would be expected to break down. He performed calculations with pions of 100–300 MeV on isospin-zero nuclei such as He, C, O;  $kR$  is then of the order of 2. Surprisingly, the model still works reasonably well.

A somewhat different situation arises when scattering nucleons on nuclei. At medium energies (150 to 1000 MeV or 550 to 1700 MeV/c), spin effects, which are usually neglected in the theory, are very important when calculating differential cross sections at small scattering angles. However, it seems worthwhile to calculate the forward scattering amplitude. The imaginary part is related by the optical theorem to the total cross section and can be checked directly by experimental data. The energy region above 1 GeV has been investigated by Franco<sup>61)</sup> using Glauber theory and he obtained very good agreement with experimental data. It is interesting to note his calculation of  $\alpha$  which he finds to be closer to zero for heavier nuclei, in agreement with the data of Schwandt below 200 MeV [ref. 48)].

Measured total cross sections as a function of energy  $E$  show a minimum around 300 MeV; the rise towards high energies is due to the onset of pion production. We have checked whether the theory is capable of reproducing the position of this minimum as well as the general shape of  $\sigma_T(E)$  in  $^2\text{H}$ , He, C, and O.

With the simplest possible assumptions listed below, the total cross section is given as a sum over  $A$  multiple scattering terms<sup>62)</sup>:

$$\sigma_A(E) = 2\pi r^2 [1 + 2r^{-2}\gamma^2(E)] \sum_{m=1}^A \binom{A}{m} (-1)^{m+1} \frac{1}{m} \left[ \frac{\sigma(E)}{2\pi r^2 [1 + 2r^{-2}\gamma^2(E)]} \right]^m \times \text{Re} [1 - i\alpha(E)]^m \quad (7)$$

$$= A\sigma - \frac{A(A-1)}{8\pi} \frac{\sigma^2}{r^2(1 + 2r^{-2}\gamma^2)} (1 - \alpha^2) + \dots, \quad (8)$$

where  $A$  is the number of nucleons in the target nucleus. [The notation differs slightly from that in ref. 62) in order not to mix the variables in this paper.]

The input quantity in the theory is the isospin averaged spin-independent nucleon-

nucleon amplitude when one is calculating the scattering of nucleons on an isospin-zero target:

$$f_{\text{NN}} = \frac{1}{2}(f_{\text{pp}} + f_{\text{pn}}) = \frac{3}{4}f(I=1) + \frac{1}{4}f(I=0), \quad (9)$$

which is approximated by an exponential in  $t$ :

$$f_{\text{NN}}(E) = \frac{ik}{4\pi} \sigma(E) [1 - i\alpha(E)] e^{-\gamma^2(E) |t|}, \quad (10)$$

where  $\sigma(E)$  is the isospin averaged NN total cross section and

$$\alpha = \alpha_{\text{NN}} = \text{Re } f_{\text{NN}} / \text{Im } f_{\text{NN}},$$

$$\gamma^2 = \text{slope parameter.}$$

The target is considered to be a pure s-state nucleus, i.e. each nucleon has an harmonic oscillator wave function in the s-state with respect to the c.m. of the nucleus. Assuming no correlations between the nucleons, the density function of the scatterer  $A$  is factorizable:

$$\rho(\mathbf{r}_1 \dots \mathbf{r}_A) = \rho(\mathbf{r}_1) \dots \rho(\mathbf{r}_A) = \left( \frac{1}{\pi r^2} \right)^{\frac{3}{2}} \exp \left\{ -\frac{1}{r^2} \left[ \sum_{i=1}^A r_i^2 \right] \right\}, \quad (11)$$

where  $r$  is related to the r.m.s. radius  $R$  of the nucleus by

$$r^2 = \frac{2}{3} R^2 \quad (12)$$

( $R$ -values are listed in table 2).

Total cross sections on  $^2\text{H}$ , He, C and O in the energy range 150–2000 MeV (550–2800 MeV/ $c$ ) were computed with the following input data:

(i) Isospin-averaged total nucleon-nucleon cross section  $\sigma_{\text{T}}(\text{NN})$ : Fig. 12 shows the actual experimental situation for nucleon-nucleon total cross-section data. For pp scattering at low energies ( $< 400$  MeV) we used the values obtained from the VPI phase-shift analyses since they agree with our pp data. At higher energies we took the precise and most recent Cambridge-Rutherford (CR) pp data of Bugg *et al.* <sup>12</sup>). For the np case we drew a smooth curve through the low-energy data of Measday and Palmieri <sup>44</sup>) and the Princeton (PPA) np data <sup>24, 25</sup>). The faint dip in the np cross section at 900 MeV is due to the minimum in  $\sigma_{\text{tot}}(I=0)$ .

(ii)  $\alpha_{\text{NN}}$ . As the calculation was performed before Grein's results were available, we used the "smoothed" curve  $\alpha(E)$  in fig. 7 up to 600 MeV and zero above. Now this could be improved a little but as  $\alpha_{\text{NN}}$  influences only the higher-order terms in eq. (7) we have not redone the calculations as the total cross-section calculation is not very sensitive to  $\alpha$  as long as  $|\alpha|$  is small with respect to 1:

example:  $\sigma_{\text{T}}(\text{He})$  at 600 MeV,

$$\alpha = 0, \quad \sigma_{\text{T}} = 118.9 \text{ mb,}$$

$$|\alpha| = 0.3, \quad \sigma_{\text{T}} = 120.2 \text{ mb.}$$

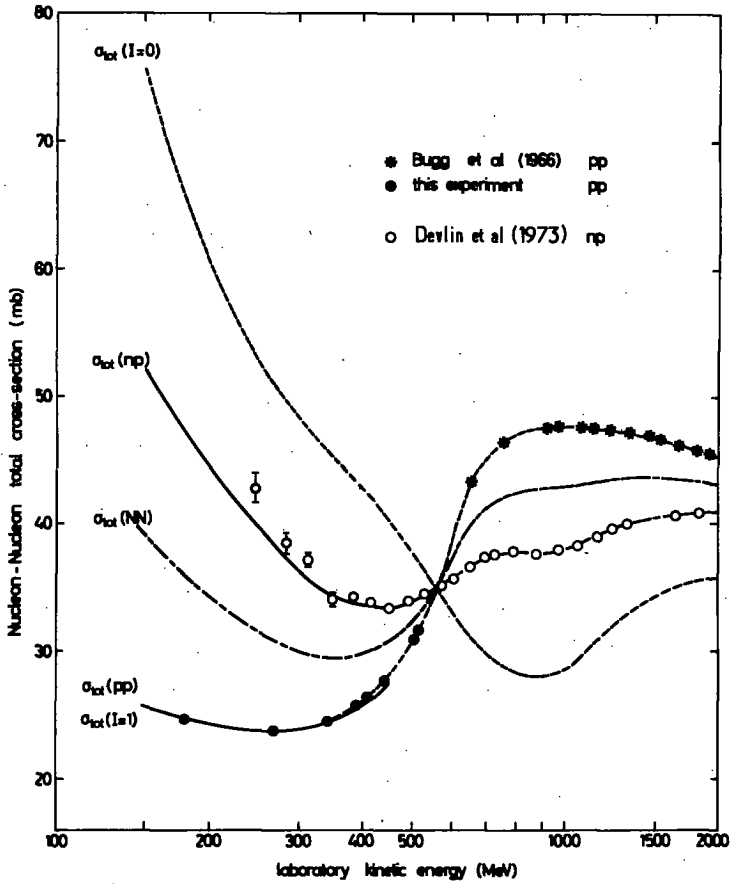


Fig. 12. Averaged total cross sections for nucleon-nucleon scattering. These data are used in the Glauber model calculation.

(iii) Slope parameter  $\gamma^2$ : The slope parameter  $\gamma^2$  at zero momentum transfer has been taken from phase shifts up to 450 MeV. At higher energies a mean  $\gamma^2 \approx 0.3 \text{ fm}^2$  fits experimental data compiled by Lasinski *et al.* <sup>63</sup>) rather well.

The results of the calculations are plotted in figs. 6, 8, 10 and 11.

$\sigma_T(pd)$  (fig. 6): in this case formula (7) reduces simply to

$$\sigma_d = 2\sigma - \frac{1}{4\pi} \sigma^2 (1 - \alpha^2) \frac{r^{-2}}{1 + 2r^{-2}\gamma^2}. \quad (13)$$

Instead of using c.m. coordinates to locate the position of the nucleons in the nucleus, the deuteron can be described with one coordinate only, the separation  $s$  of the two nucleons. Assuming again a Gaussian-type density distribution in  $s$ , the parameter  $r^{-2}$  in eq. (13) equals the expectation value of the inverse square separation <sup>64</sup>):  $r^{-2} = \langle s^{-2} \rangle$ .

At low energies the impulse approximation (IA) fits the data almost perfectly. In any case, the double scattering correction is small ( $\leq 2\%$ ) because both  $\gamma^2$  and  $\alpha$  increase towards low energies and therefore suppress the second term.

Furthermore, the charge exchange contribution can easily be taken into account by replacing  $\sigma^2$  in the double scattering term by

$$\sigma_{pp}\sigma_{np} - \frac{1}{2}(\sigma_{np} - \sigma_{pp})^2 \quad (14)$$

charge exchange term

It reduces this term by about 20% at 200 MeV, 6% at 400 MeV, and has no effect at 560 MeV where  $\sigma_{np} = \sigma_{pp}$ .

At high energies we are faced with the situation where the nd data from the PPA group disagree by more than 1.5% with the pd data measured by the CR group. A recent measurement<sup>13)</sup> of the pd total cross section at 3 GeV/c yields a result which is lower than the CR set by 1.2 mb; thus we conclude that there may be a systematic error of this amount in the CR data. The nd and pd cross sections should be equal if charge symmetry is valid. We have varied the parameter  $\langle s^{-2} \rangle$  and found that  $\langle s^{-2} \rangle = 0.2 \text{ fm}^{-2}$  fits the CR data remarkably well. It needs a value of  $0.33 \text{ fm}^{-2}$  in order to come closer to the PPA data. However, the over-all agreement in the whole energy region is much worse. The correct value for the mean inverse square separation  $\langle s^{-2} \rangle$  is still not known; it may vary between 0.2 and  $0.4 \text{ fm}^{-2}$  [refs. 12, 65)].

Other Glauber model calculations have been made by Devlin *et al.*<sup>25)</sup> and by Alberi and Gregorio<sup>66)</sup>. To illustrate these calculations more clearly we use the relation

$$\sigma_d = \sigma_{np} + \sigma_{pp} - \Delta\sigma, \quad (15)$$

where  $\Delta\sigma$  is thus the shadow correction of Glauber, i.e. the second term in eq. (8). In fig. 13 we illustrate our experimental values for  $\Delta\sigma$  using our pd and pp cross sections together with np values taken from the literature<sup>3, 25)</sup>. Details are included in table 4. We illustrate the calculation of Alberi and Gregorio which gives results which are similar to our own and those of Devlin *et al.* We see that  $\Delta\sigma$  is calculated to be between 3 and 4 mb in our energy region whereas experimentally it is consistent with zero. The Fermi motion of the target nucleons was not included in the original calculations and this tends to fill in the dip in  $\sigma_T$  at 300 MeV by about 1 mb and we have given an indication of this correction in fig. 13 as well. There is still however a discrepancy of 2 or 3 mb which remains unexplained.

$\sigma_T(p^4 \text{ He, C, O})$  (figs. 8, 10 and 11): The comparison of our Glauber model calculations with experimental data shows three important facts:

(i) The depths of the minima of the calculated total cross sections equal the experimental minimum values, which is remarkable since the multiple scattering corrections compared to the impulse term (IA) are as large as 20–30%.

(ii) The multiple scattering terms shift the minimum of the NN total cross section,

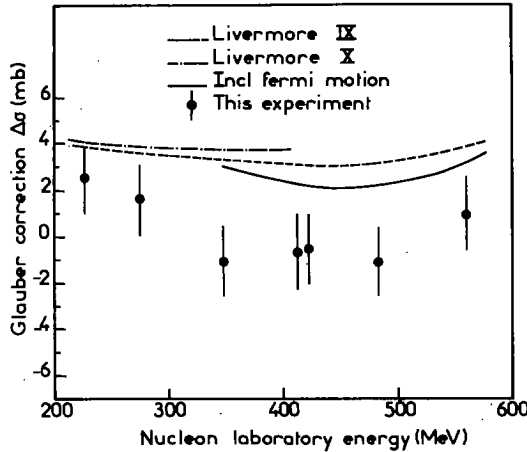


Fig. 13. Calculation of the Glauber shadow correction for the deuteron i.e.  $\sigma_{pd} = \sigma_{np} + \sigma_{pp} - A\sigma$ . Calculations are those of Alberi and Gregorio <sup>66</sup>.

which is at 335 MeV, towards higher energies. This experimental minima, however, are at lower energies (280–300 MeV) and disagree with the theory by 70–100 MeV. The same theoretical approach predicts a shift towards lower energies for the  $\pi$ -nucleon (3, 3) resonance in  $\pi$ -nucleus total cross sections <sup>67</sup>), which is observed experimentally.

(iii) The theoretical curve has roughly the correct shape as a function of energy, and agrees fairly well at higher energies where any structure in NN total cross sections disappears.

To try and understand the discrepancies we have considered the <sup>12</sup>C and <sup>16</sup>O nucleus to be composed of three or four  $\alpha$ -particles, respectively, and have introduced into the Glauber formalism a  $p^4\text{He}$  amplitude similar to the expression (10). We used our experimental  $\sigma_T$  and  $\alpha$ -values for  $p^4\text{He}$ , whereas  $\gamma^2 \approx 1.05 \text{ fm}^2$  was taken from differential cross section data. The results are given in figs. 10 and 11 and they reproduce the experimental data in <sup>12</sup>C and <sup>16</sup>O fairly well. Thus once  $p^4\text{He}$  scattering is properly understood it should be easy to encompass other nuclei. A more complete  $\alpha$ -model calculation has been performed by Ahmad and Khan <sup>68</sup>) for <sup>12</sup>C and they obtained an even better agreement with our data.

Since Glauber theory still works well at low energies (pd data,  $\pi$ -nucleus data) we discuss briefly various effects, not considered in the theory, which may explain the energy shift of total cross-section minima <sup>69</sup>). We have not made any detailed calculations.

Fermi motion: The NN total cross-section curve is rather symmetric around its minimum, so the effect of Fermi motion on the  $A\sigma$  term in eq. (8) is that it just smoothes the structure. However, as has been pointed out by Ahmad and Khan <sup>68</sup>) the parameter  $\gamma$  can have an energy dependence so the effects of Fermi motion can be quite complex. Other effects are: non-Gaussian form of the elementary NN

amplitude; strong contribution of spin effects; kinematical problems; finite integration limits when integrating over the momentum transfer  $q$ ; back-scattering; re-scattering on the same nucleon; isospin 1 and 0 amplitudes have to enter the theory explicitly since they differ considerably at low energies – the  $\alpha$ -values get close to 1, i.e. delicate cancellations of higher-order terms may happen; non-Gaussian single-particle density in the nucleus (surface effects); correlations between nucleons in the nucleus.

It needs a detailed theoretical investigation in order to establish which effects contribute dominantly to the observed large energy shift. It could easily be that at different energies different effects are dominant. We note that just such a study has been made by Young and Wong for  $p^4\text{He}$  elastic scattering <sup>70</sup>).

### 5.5. CHARGE SYMMETRY

A direct test of charge or isospin symmetry is possible by comparing proton and neutron total cross sections on an isospin-zero target as a function of energy. Since charge symmetry is believed to hold by 0.5% to 1% [ref. <sup>28</sup>)] it needs rather high precision data in order to be sensitive to such small differences. At present it is a difficult task to measure proton total cross sections to an accuracy of better than 0.5% since the biggest uncertainties are still due to Coulomb and Coulomb-nuclear interference corrections at least in the energy region of a few hundred MeV. When new differential cross-section data become available, the situation may change. For neutron total cross sections, more often the problem of statistics and systematic errors in the apparatus of the order of 0.5–1% become important.

With the actual precision of total cross sections on nuclei such as  $^{12}\text{C}$  or  $^{16}\text{O}$  it is only possible to conclude that charge symmetry is valid to about 6%. However, our data on the deuteron agree, within error, with the most recent PPA nd total cross sections. Errors on these experiments are 1% and 0.4% respectively for the deuteron cross section of which about half can be attributed to the  $n\bar{n}$  and  $pp$  cross section. Because of the large discrepancy of more than 1.5% at higher energies (probably due to systematic errors in the experiments) it is again reasonable to claim only about a 5% confirmation of charge symmetry.

## 6. Conclusions

The experimental data presented here have filled in several lacunae in the knowledge of total cross sections at intermediate energies, as well as arbitrating between discrepant results. The proton-proton data are an important contribution to the knowledge of the nucleon-nucleon interaction as they provide a dependable normalization through this energy region. The proton-deuteron data are interesting tests of Glauber theory as well as a good check on charge symmetry in nuclear forces but some strong discrepancies exist. The experimental technique could easily provide

more precise measurements and these would be quite valuable in the proton-deuteron case. However further data on the elastic differential cross sections in neutron-proton scattering would be needed to improve our confidence in the reliability of the phase shifts to reproduce accurately the Coulomb-nuclear interference region. For the pp case there is current interest in this problem<sup>38</sup>), but unfortunately data on deuterium are not available.

The proton-nucleus data are a useful check on neutron total cross-section results but the latter are considerably easier to obtain reliably. However we obtained, as a by-product, values of  $\alpha$ , the real to the imaginary part of the forward spin independent scattering amplitude. They could be a valuable constraint on optical model calculations and our review of the existing analyses shows that not enough data exist for small angle scattering with the result that there is some lack of sensitivity to the ratio of the real to the imaginary part of the optical model potentials.

We are very grateful to Dr. E. G. Michaelis at CERN, for his interest and support of us during this experiment. P. S. and M. P. wish to thank Professor J. P. Blaser (SIN and ETH Zurich) and B. F. and C. R.-S. wish to thank the University of Grenoble for the opportunity of working at CERN. D. F. M. wishes to acknowledge the hospitality of CEN Saclay where the manuscript was completed. In the analysis of the data we enjoyed considerable help from many people, in particular we wish to thank Dr. M. P. Locher for his illuminating discussions on various topics and especially the dispersion relation calculations; Professor R. A. Arndt and Dr. F. Lehar for providing us with data from their phase-shift analyses; B. C. Clark and P. Schwandt for calculating the forward scattering amplitudes from their optical model analyses; and Dr. G. Alberi and Dr. M. A. Gregorio for sending us the numerical results of their proton-deuteron calculations.

### References

- 1) P. Schwaller, Ph.D. Thesis, ETH Zürich;  
P. Schwaller, B. Favier, D. F. Measday, M. Pepin, P. U. Renberg and C. Richard-Serre, CERN 72-13 (1972), Scientific Information Service, CERN, 1211 Geneva 23, Switzerland
- 2) P. Schwaller, M. Pepin, D. F. Measday, P. U. Renberg, B. Favier and C. Richard-Serre, Phys. Lett. **35B** (1971) 243
- 3) F. F. Chen, C. P. Leavitt and A. M. Shapiro, Phys. Rev. **103** (1956) 211
- 4) V. P. Dzheleпов, V. I. Moskalev and S. V. Medved', Dok. Akad. Nauk SSSR **104** (1955) 380
- 5) M. J. Longo, J. A. Helland, W. N. Hess, B. J. Moyer and V. Perez-Mendez, Phys. Rev. Lett. **3** (1959) 568
- 6) M. J. Longo and B. J. Moyer, Phys. Rev. **125** (1962) 701
- 7) O. Chamberlain, G. Pettingill, E. Segrè and C. Wiegand, Phys. Rev. **93** (1954) 1424;  
G. H. Pettingill, UCRL-2808 (1954)
- 8) O. Chamberlain, E. Segrè and C. Wiegand, Phys. Rev. **81** (1951) 284; **83** (1951) 923
- 9) H. G. de Carvalho, Phys. Rev. **96** (1954) 398
- 10) V. M. Guzhavin, G. K. Kliger, V. Z. Kolganov, A. V. Lebedev, K. S. Marish, Yu. D. Prokoshkin, V. T. Smolyankin, A. P. Sokolov, L. M. Soroko and Ts'ui Wa-Ch'uang, JETP (USSR) **46** (1964) 1245 [JETP (Sov. Phys.) **19** (1964) 847]

- 11) J. Marshall, L. Marshall and A. V. Nedzel, *Phys. Rev.* **91** (1953) 767
- 12) D. V. Bugg, D. C. Salter, G. H. Stafford, R. F. George, K. F. Riley and R. J. Tapper, *Phys. Rev.* **146** (1966) 980
- 13) R. J. Abrams, R. L. Cool, G. Giacomelli, T. F. Kycia, B. A. Leontic, K. K. Li and D. N. Michael, *Phys. Rev.* **D1** (1970) 2477
- 14) K. F. Riley, *Phys. Rev.* **D1** (1970) 2481
- 15) R. Goloskie and J. N. Palmieri, *Nucl. Phys.* **55** (1964) 463
- 16) G. F. Cox, G. H. Eaton, C. P. Van Zyl, O. N. Jarvis and B. Rose, *Nucl. Phys.* **B4** (1967) 353
- 17) D. E. Young and L. H. Johnston, *Phys. Rev.* **119** (1960) 313
- 18) M. R. Wigan, R. A. Bell, P. J. Martin, O. N. Jarvis and J. P. Scanlon, *Nucl. Phys.* **A114** (1968) 377
- 19) M. H. MacGregor, R. A. Arndt and R. M. Wright, *Phys. Rev.* **182** (1969) 1714
- 20) R. A. Arndt, R. H. Hackman and L. D. Roper, *Phys. Rev.* **C9** (1974) 555
- 21) R. A. Arndt, R. H. Hackman and L. D. Roper, *Phys. Rev.* **C15** (1977) 1002; 1021
- 22) F. Lehar and J. Bystricky, private communication
- 23) R. A. Arndt, private communication
- 24) R. E. Mischke, T. J. Devlin, W. Johnson, J. Norem, K. Vosburgh and W. Schimmerling, *Phys. Rev. Lett.* **25** (1970) 1724
- 25) T. J. Devlin, W. Johnson, J. Norem, K. Vosburgh, R. E. Mischke and W. Schimmerling, *Phys. Rev.* **D8** (1973) 136
- 26) C. Wilkin, C. R. Cox, J. J. Domingo, K. Gabathuler, E. Pedroni, J. Kohlin, P. Schwaller and N. W. Tanner, *Nucl. Phys.* **B62** (1973) 61
- 27) E. Pedroni, K. Gabathuler, J. Arvieux, J. J. Domingo, P. Gretillat, W. Hirt, C. H. Q. Ingram, J. Piffaretti, P. Schwaller, N. W. Tanner and C. Wilkin, *Proc. Zürich Conf.* paper E11 (1977)
- 28) E. M. Henley, *Isospin in nuclear physics*, ed. D. H. Wilkinson (North-Holland, Amsterdam, 1969); E. M. Henley and G. A. Miller, *Meson theory charge dependent nuclear forces*, in *Mesons in nuclei*, ed. M. Rho and D. H. Wilkinson (North-Holland), to be published
- 29) P. U. Renberg, D. F. Measday, M. Pepin, P. Schwaller, B. Favier and C. Richard-Serre, *Nucl. Phys.* **A183** (1972) 81
- 30) A. M. Saperstein, *Phys. Rev. Lett.* **30** (1973) 1257
- 31) M. P. Locher, *Nucl. Phys.* **B36** (1972) 634
- 32) R. J. Tapper, *NIRL/R/95* (1965)
- 33) R. B. Stewart and V. J. Johnson, ed., *Compendium of properties of materials at low temperature*, technical report 60-56, part 1, Wright Air Development Division, Wright Patterson Air Force Base, Ohio
- 34) C. Serre, *CERN 67-5* (1967)
- 35) J. F. Janni, *Air Force Weapons Laboratory Technical Report*, AFWL-TR-65-150 (1966)
- 36) W. H. Barkas and M. J. Berger, *NAS-NRC publication* (1964) 1133
- 37) W. Grein, *Nucl. Phys.* **B131** (1977) 255
- 38) D. Aebischer, B. Favier, L. G. Greeniaus, R. Hess, A. Junod, C. Lechanoine, J. C. Niklès, D. Rapin, C. Richard-Serre and D. W. Werren, *Phys. Rev.* **D13** (1976) 2478
- 39) J. Bystricky and F. Lehar, *Nucleon-nucleon scattering data*, *Physics Data 11-1 ZAED* (1978)
- 40) G. Giacomelli, *CERN-HERA 69-3* (1969)
- 41) V. S. Barashenkov, *Interaction cross sections of elementary particles* (1968) (English translation: IPST Press, Jerusalem)
- 42) J. D. Hansen, D. R. O. Morrison, N. Tovey and E. Flamino, *CERN-HERA 70-2* (1970)
- 43) O. Benary, L. R. Price and G. Alexander, *UCRL 20 000 NN* (1970)
- 44) D. F. Measday and J. N. Palmieri, *Nucl. Phys.* **85** (1966) 129
- 45) D. F. Measday and J. N. Palmieri, *Nucl. Phys.* **85** (1966) 142
- 46) W. Schimmerling, T. J. Devlin, W. Johnson, K. G. Vosburgh and R. E. Mischke, *Phys. Lett.* **37B** (1971) 177
- 47) W. Schimmerling, T. J. Devlin, W. W. Johnson, K. G. Vosburgh and R. E. Mischke, *Phys. Rev.* **C7** (1973) 248
- 48) P. Schwandt, *IUCF data*, private communication
- 49) A. H. Cromer and J. N. Palmieri, *Ann. of Phys.* **30** (1964) 32
- 50) O. N. Jarvis, *Nucl. Phys.* **79** (1966) 305

- 51) O. N. Jarvis, M. Shah and C. Whitehead, *Nucl. Phys.* **184** (1972) 615
- 52) B. C. Clark, R. L. Mercer, D. G. Ravenhall and A. M. Saperstein, *Phys. Rev.* **C7** (1973) 466
- 53) L. G. Arnold, B. C. Clark and R. L. Mercer, *Nuovo Cim. Lett.* **18** (1977) 151
- 54) B. C. Clark and R. L. Mercer, private communication
- 55) L. I. Schiff, *Quantum mechanics* (McGraw-Hill, New York, 1955) p. 169
- 56) A. Ingemarsson and G. Tibell, *Phys. Scripta* **4** (1971) 235
- 57) L. Ray and W. R. Coker, *Phys. Rev.* **C16** (1977) 340
- 58) G. Eckart and M. K. Weigel, *J. of Phys.* **G2** (1976) 487
- 59) J. N. Palmieri and R. Goloskie, *Nucl. Phys.* **59** (1964) 253
- 60) C. Wilkin, *Proc. Banff Summer School on intermediate energy nuclear physics* (Aug. 1970) (published by Department of Physics, The University of Alberta, Alberta)
- 61) V. Franco, *Phys. Rev.* **C6** (1972) 748
- 62) B. Margolis and C. S. Lam, *Nuclear and particle physics* (Benjamin, NY, 1968) p. 469
- 63) T. Lasinski, R. Levi Setti, B. Schwarzschild and P. Ukleja, *Nucl. Phys.* **B37** (1972) 1
- 64) V. Franco and R. J. Glauber, *Phys. Rev.* **142** (1966) 1195
- 65) A. A. Carter, K. F. Riley, R. J. Tapper, D. V. Bugg, R. S. Gilmore, K. M. Knight, D. C. Salter, G. H. Stafford, E. J. N. Wilson, J. D. Davies, J. D. Dowell, P. M. Hattersley, R. J. Homer and A. W. O'Dell, *Phys. Rev.* **168** (1968) 1457
- 66) G. Alberi and M. A. Gregorio, *Nuovo Cim. Lett.* **5** (1972) 585;  
G. Alberi, L. Bertocchi and M. A. Gregorio, *Nuovo Cim.* **10A** (1972) 37; and private communication
- 67) M. P. Locher, O. Steimann and N. Straumann, *Nucl. Phys.* **B27** (1971) 598
- 68) I. Ahmad and Z. A. Khan, *Nucl. Phys.* **A274** (1976) 519
- 69) T. E. O. Ericson, K. Gottfried, O. Kofoed-Hansen, M. P. Locher and C. Wilkin, private communication
- 70) S. K. Young and C. W. Wong, *Phys. Rev.* **C15** (1977) 2146
- 71) H. A. Bethe, *Ann. of Phys.* **3** (1958) 190
- 72) M. D. Cooper and M. B. Johnson, *Nucl. Phys.* **A260** (1976) 352
- 73) R. F. Frosch, J. S. McCarty, R. E. Rand and M. R. Yearian, *Phys. Rev.* **160** (1967) 874